

Urban Ecological Quality Assessment Based on Remote Sensing Data in African Context – A Case Study of Tangier City (Morocco, NW Africa)

Mounia Tahiri^{1*}, Hicham Bahi², Tarik Bouramtane¹, Anass Malah²,
Anas Sabri², Ismail Mohsine¹, Ilias Kacimi¹

¹ Laboratory of Geosciences, Water and Environment, Department of Earth Sciences, Faculty of Sciences, Mohammed V University in Rabat, Morocco

² School of Architecture, Planning and Design, Mohammed VI Polytechnic University, Benguerir, Morocco

* Corresponding author's e-mail: m.tahiri@um5r.ac.ma

ABSTRACT

Climate change, combined with rapid urbanization, can face many challenges in achieving urban ecological sustainability, especially in developing countries. Due to the lack of valuable data, measuring the negative impact of this urban environmental damage, particularly in African cities, is however difficult to investigate. In this context, this research proposes an efficient index, including environmental, societal, and topographic indicators, extracted from remote sensing data, to evaluate the spatial ecological vulnerability of Tangier city in Morocco. This composite index, called the Urban Ecological Quality Index (UEQI), was developed for 2002, 2013, and 2023 in the spring season, using the Principal Component Analysis (PCA) as a multivariate statistical technique. Furthermore, the spatial autocorrelation analysis of the UEQI was performed to study the correlation between the index values and its surroundings, using Global Moran's I and Local Moran's I test statistics. The results show that on the one hand, zones located in the center of the city kept poor ecological quality in the three studied years, where the lack of green spaces and the high population density are the main reasons for this bad state. On the other hand, climate variability, such as precipitation change, directly affects the ecological quality of Tangier city. In fact, from 2002 to 2013, due to Morocco's increased precipitation during this decade, the UEQI improved in 36%, unchanged in 50%, and degraded in 14% of the study area. However, from 2013 to 2023, with more than 52% degraded UEQI, the ecological quality of the city was affected by drought periods, which have been more frequent and intense in this decade, especially in green areas and agricultural land.

Keywords: ecological quality, multivariate statistic, remote sensing, climate change, urbanization, Morocco.

INTRODUCTION

Since the past half century, the globe has grown more urbanized, especially in developing nations, reaching 56% of the urban population in 2021 [World Bank, 2021]. By 2050, cities are expected to house 70% of the world's population [UN, 2007]. In 2022, the population of African countries exceeded one billion people, with around 44% living in metropolitan areas [UN, 2010, 2022]. According to several previous studies, this urbanization increase is the main cause of many environmental problems such as vegetation

decrease and agricultural land loss [López et al., 2001], impervious urban rising [Weng, 2012], evapotranspiration decrease [Chai et al., 2022], environmental pollution [Liu et al., 2022], urban heat island development [Bahi et al., 2016], and many others. In Morocco (Northwest of Africa), very few published studies [Malah et al., 2022; Malah & Bahi, 2022] attempt to develop a composite index to evaluate the ecological quality in an urban context by combining indicators from different aspects such as environmental, socio-economic, topographic, etc., especially in Moroccan northern cities. Tangier, the main economic

city, has recently experienced an economic rise in power through the implementation of many structuring projects. As a result, the urban ecological quality of these northern cities needs to be assessed through accessible techniques to inform the general population of how well their living environment is maintained.

To evaluate the general ecological state in an urban environment, it is necessary to quantify the relation between the urban and social features of a location [Merschdorf et al., 2020]. Furthermore, urban ecological quality is a complicated parameter fluctuating in time and space. It is the result of interactions between environmental factors, such as greenness, soil moisture, land temperature, etc., and human activities that can have a high or low weight on life's quality [Kamp et al., 2003]. In an urban context, objective and subjective indicators are frequently used to evaluate the quality of life in cities [Pacione, 2003]. The first approach consists of quantifiable indicators that describe the conditions in which residents live and work objectively, while subjective indicators are used to explain how people see and assess the world around them [Kazemzadeh-Zow et al., 2018].

Assessing the urban ecological quality using the objective approach has been the aim of several previous studies [Joseph et al., 2014; Assaye et al., 2017; Musse et al. 2018; Pramanik et al., 2021; Sousa et al., 2021; Roy et al., 2022], where the indicators were mainly extracted from satellite images, census data or observation measures. Since remote sensing data became publicly available providing most elements of urban ecological states, particularly in African cities due to the lack of spatial data and the difficulty in information access, the objective methodology to assess the ecological quality of Tangier city was selected in this study.

Therefore, this study aims to propose, for the first time in a Moroccan northern city and by using only remote sensing data, an efficient approach to develop a composite index namely the Urban Ecological Quality Index (UEQI) for assessing ecological quality in an urban context. The years 2002, 2013, and 2023 were selected to analyze the spatio-temporal changes in the ecological quality of the study area. To achieve this, three types of indicators (environmental, societal, and topographic) derived from remote sensing products were integrated by a Principal Component Analysis (PCA) to compute the UEQI developed index. This study's findings attempt to identify the parameters affecting the ecological

quality of the study area, especially where the areas with poor quality are located within the city.

STUDY AREA

Located in Northwest Morocco (35°45' 34.074" N, 5°50'2.234" W) 14 km from the southern Spanish coast, Tangier city, the study area in this research, is considered the gateway to Africa along the Strait of Gibraltar (Fig. 1). As the capital of the Tangier-Tétouan-Al Hoceima (TTA) region, Tangier consists of four urban districts: Tangier Medina (TM), Charf Souani (CS), Charf Mghogha (CM), and Beni Makada (BM). Furthermore, the city has a Mediterranean climate, influenced by its proximity to the Atlantic Ocean. The seasons are distinct, with mild, rainy winters and hot, sunny summers. The average annual temperature is 17.5°C and the average precipitation ranges from 600 to 1000 mm per year [Bouramtane et al., 2021]. Additionally, according to the land cover map for the year 2023, Tangier is surrounded to the east and west by urban forest and grassland, which has resulted in the city expanding to the south.

Based on the last Moroccan census in 2014, the population of Tangier represented 2.78% of the Moroccan population. By 2030, Tangier's population is expected to reach 3.42% of the national population [High Commissioner for Planning, 2014, 2018]. This population growth can be explained by its economic potential mainly due to its proximity to Europe and its multiple economic zones including two maritime ports, Tangier-City and Tangier-Med ports. As a result, Tangier has become the second economic hub of Morocco in the last decade, just after Casablanca city.

METHODOLOGY

Data pre-processing

This section presents the methodology adopted (Fig. 2) for developing the UEQI index in Tangier city for the years 2002, 2013, and 2023. Three types of indicators: environmental, societal, and topographic (Table 1) were selected in this work given their impact on the urban ecological quality, according to previous studies [Musse et al. 2018; Pramanik et al., 2021; Sousa et al., 2021]. Seven spectral indexes were chosen as

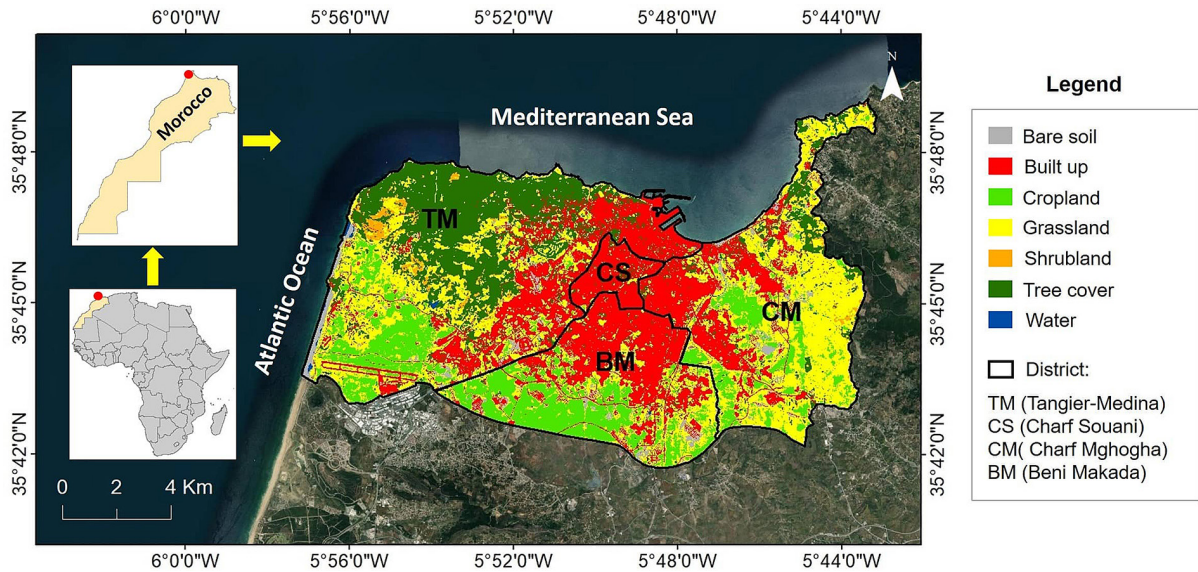


Fig. 1. Location of the study area (north of Morocco)

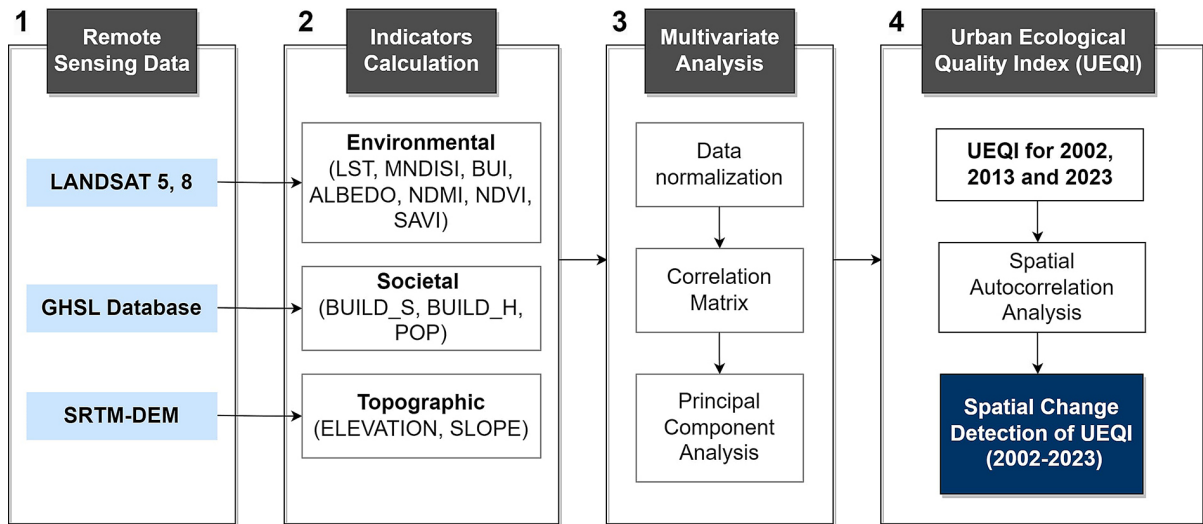


Fig. 2. Flowchart representing the UEQI process

environmental indicators (Table 1): Land Surface Temperature (Eq. 1), Modified Normalized Difference Impervious Surface Index (Eq. 2), Build-up Index (Eq. 3), Surface Albedo (Eq. 4), Normalized Difference Vegetation Index (Eq. 5), Soil Adjusted Vegetation Index (Eq. 6), and Normalized Difference Moisture Index (Eq. 7). These indicators are related to surface temperature, vegetation, soil humidity, albedo, and impervious surfaces. The spring season was selected for the images to prevent the influence of seasonal variations and differences in rainfall during the three years. Landsat 5 and 8 data were used to extract the environmental indicators. The satellite data was downloaded from the United States Geological Survey

(USGS), with zero cloud cover within the study area boundary. Radiometric and atmospheric corrections were applied to the satellite images to improve the accuracy of their reflectance calculations. The societal indicators, which are building surface [Pesaresi & Politis, 2022a], building height [Pesaresi & Politis, 2022b], and residential population [Schiavina et al., 2022], were extracted from the spatial framework of the Global Human Settlement Layer (GHSL), established by the European Commission. Since GHSL data (available since 1975) have a temporal step of 5 years, each societal image used for this study (2002, 2013, and 2023) was calculated based on the average of data from the years before and after. In addition, these

Table 1. Indicators selected for the urban environmental quality assessment

Indicator	Formula	No.	Description	Units	References
Environmental indicator					
Land surface temperature (LST)	$LST = \frac{T_B}{1 + \left(\frac{\lambda * T_B}{\alpha}\right) * \ln(\epsilon)}$	Eq. 1	T_B is the brightness temperature, λ is the wavelength of emitted radiance, $\alpha = 1,438 \times 10^{-2}$ mK, ϵ is soil emissivity	°C	(Artis & Carnahan, 1982)
Modified normalized difference impervious surface index (MNDISI)	$MNDISI = \frac{T_s - \frac{MNDWI + \rho_{NIR} + \rho_{SWIR}}{3}}{T_s + \frac{MNDWI + \rho_{NIR} + \rho_{SWIR}}{3}}$	Eq. 2	T_s is the land surface temperature, MNDWI is the modified normalized difference water index, ρ is the spectral reflectance of the corresponding band	Unitless	(Xu, 2006; Sun et al., 2017)
Built-up index (BUI)	$BUI = NDBI - NDVI$	Eq. 3	NDBI is the normalized difference built-up index, NDVI is the normalized difference vegetation Index	Unitless	(He et al., 2010; Tucker, 1979)
Land surface Albedo (ALBEDO)	$ALBEDO = \alpha_{short} = 0.365\rho_2 + 0.13\rho_4 + 0.373\rho_5 + 0.085\rho_6 + 0.072\rho_7 - 0.0018$	Eq. 4	α_{short} is the total short wave Albedo, ρ is the spectral reflectance of the corresponding band	Unitless	(Liang, 2003)
Normalized difference vegetation index (NDVI)	$NDVI = \frac{\rho_{NIR} - \rho_{RED}}{\rho_{NIR} + \rho_{RED}}$	Eq. 5	ρ is the spectral reflectance of the corresponding band	Unitless	(Tucker, 1979)
Soil adjusted vegetation index (SAVI)	$SAVI = \left(\frac{\rho_{NIR} - \rho_{RED}}{\rho_{NIR} + \rho_{RED} + L}\right) * (1 + L)$	Eq. 6	ρ is the spectral reflectance of the corresponding band, L is a brightness correction factor	Unitless	(Huete, 1988)
Normalized difference moisture index (NDMI)	$NDMI = \frac{\rho_{NIR} - \rho_{SWIR}}{\rho_{NIR} + \rho_{SWIR}}$	Eq. 7	ρ is the spectral reflectance of the corresponding band	Unitless	(Gao, 1996)
Societal indicator					
Building surface (BUILD_S)	-	-	Spatial distribution of the built-up surfaces, expressed as number of square meters	m ²	(Pesaresi & Politis, 2022b)
Building height (BUILD_H)	-	-	Spatial distribution of the building heights	m	(Pesaresi & Politis, 2022a)
Residential population (POP)	-	-	Number of inhabitants per cell	Inhabitant per cell	(Schiavina et al., 2022)
Topographic indicator					
Elevation	-	-	Elevation of the pixel	m	(Davies et al., 2008)
Slope	-	-	Measure of steepness or the degree of inclination of a feature relative to the horizontal plane	Degree	(Carrión-Mero et al., 2021)

indicators were resampled to a 30m resolution to be adapted to the spatial resolution of the other parameters. Elevation and slope, the topographic indicators, were extracted from the NASA Shuttle Radar Topographic Mission (SRTM) - Digital Elevation Model (DEM), with a resolution of 30m [Farr & Kobrick, 2000].

Urban ecological quality index

To combine all the indicators into a single index, Principal Components Analysis were used as a weighting technique that reduces correlated input variables to uncorrelated components based on the total variance they explain [Lo, 1997].

Before proceeding with PCA, Pearson’s correlation was determined to investigate the correlations between the twelve indicators. For UEQI development, only principal components with eigenvalues greater than 1 were kept [Kaiser, 1960; Lo, 1997]. Additionally, the data suitability was examined using the communality of each indicator and two statistics measures such as Kaiser Meyer Olkin (KMO) and Bartlett’s tests [Nardo et al., 2005]. Furthermore, the indicator’s loadings in the retained components were used to interpret the relationships between the indicators and the components. Once the most explicative components were selected, the UEQI Index was calculated using the score and the variance of each component using the following equation [Li, 2007] (8):

$$UEQI = \sum_{i=1}^n f_i w_i \quad (8)$$

where: n – the total number of extracted components, f_i – the component’s score, and w_i – the variance percentage explained by component i . UEQI values were then normalized and classified into five classes to improve the readability of the results between the three years studied.

Spatial autocorrelation analysis of the UEQI

To examine the possible correlation between the ecological quality of a feature and its enclosing area, the spatial autocorrelation analysis of the UEQI model can be used to characterize geographically the distribution of the index in our study area [Martin, 1996]. For this purpose, Global Moran’s I (Eq. 9) and Local Moran’s I (Eq. 10) test statistics were used in this research. Global Moran’s I value ranges from -1 to 1; values closer to 1 indicate a strong positive autocorrelation of the index. Local Moran’s I maps identify the spatial cluster dependency between variables and their surroundings. Both indices are calculated as follows [Anselin, 1995]:

$$Global\ Moran's\ I = \frac{n * \sum_{i=1}^n \sum_{j=1}^n W_{ij} (x_i - \bar{x})(x_j - \bar{x})}{(\sum_{i=1}^n \sum_{j=1}^n W_{ij}) * \sum_{i=1}^n (x_i - \bar{x})^2} \quad (9)$$

$$Local\ Moran's\ I = \frac{(x_i - \bar{x}) * \sum_{j=1}^n W_{ij} (x_j - \bar{x})}{\sum_{i=1}^n (x_i - \bar{x})^2} \quad (10)$$

where: n – the total number of spatial elements, x_i and x_j – the UEQI values of the elements i and j , \bar{x} – the average value of UEQI in the study area; W_{ij} – the spatial weight between

the elements i and j (equal to 0 for elements that are not adjacent, and 1 otherwise).

RESULTS

Initial data exploration

A spatial distribution was conducted to summarize the indicators used in this study for the years 2002 and 2023 (Fig. 3). Since their range values are different, all the data were normalized on the same scale [0,1] enabling comparison between them. In 2002, the spatial distribution of environmental indicators demonstrated a visible distinction between the superficial and vegetal zones of Tangier city. This is due to the greater concentration of impermeable surfaces in the city’s center. The NDVI and the SAVI display high vegetation cover values in the forest of northwest Tangier and the surrounding agricultural areas. Despite this, the southeast and southwest of the study area experience higher thermal values due to the presence of significant mineralized and impermeable surfaces, such as industrial and airport zones, which are resistant to the Mediterranean climate’s precipitation in that region.

However, in 2023, the expansion of the building and impermeable surfaces caused a decrease in the vegetation values in the south of the city. Beni Makada district, the southern district of Tangier, was the most affected by this diminution of green space. Regarding the soil temperature, the thermal values increased mainly in the southern part of the four districts, whereas in 2002 the values were fresher during the same season.

The geographical dispersion of societal data shows that built-up zones are located in the urban area of the city with the main concentration in the industrial zone of Mghogha, which is home to multi-sectoral companies. Also, the high-rise buildings north of the city, which increased in 2023, correspond to malls, hotels, or business centers along the coast of Tangier Bay. During both years, the population density remained concentrated in the north of the Beni Makada district, where the type of habitat is mainly traditional houses. The topography of Tangier city is dominated by large areas of hills, with an altitude of less than 350 m, creating a valley with a small depth. In addition, the slope gradient varies in the range of 0 ~ 50°, where the high values are located on the northwest side of the city.

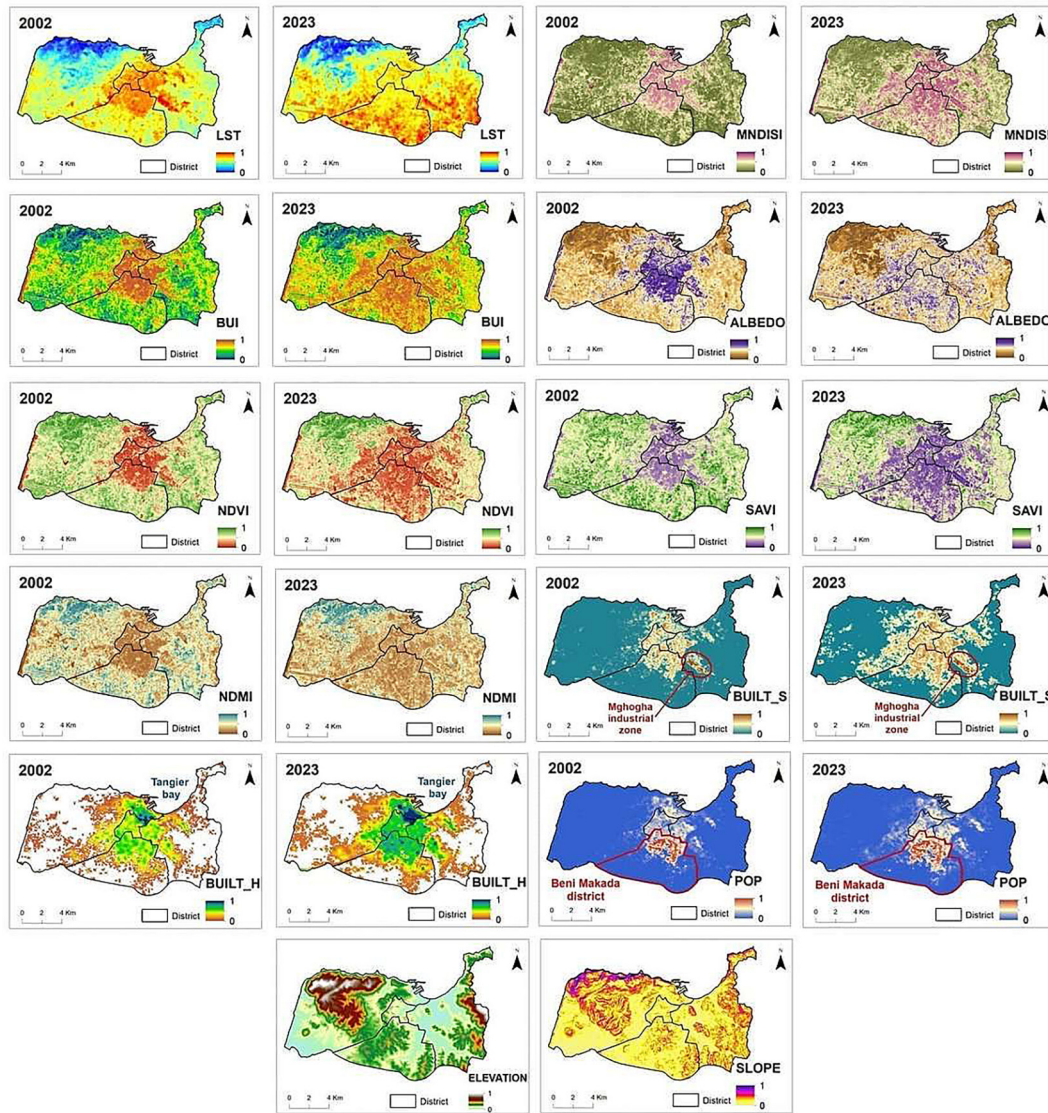


Fig. 3. Spatial distribution of the indicators (environmental, societal, and topographic) for the years 2002 and 2023 in Tangier city

Statistical exploration

To assess the urban ecological quality of Tangier city for 2002, 2013, and 2023 using Principal Component Analysis, a statistical exploration of the indicators was performed using a Pearson correlation analysis to examine their interdependence. Taking 2023 as an example (Fig. 4), the results show that the Pearson correlation coefficients (r) indicate a strong positive correlation between LST and MNDISI, ALBEDO, and BUI (respectively $r = 0.736, 0.798, \text{ and } 0.827$). However, these indicators and the vegetative indices (NDVI, SAVI, and NDMI), are negatively correlated, with r values that range from -0.995 to -0.726 . The presence of impervious surfaces, added to the lack of greenness, increases the

surface temperature in urban cities. Furthermore, the analysis indicates that topographic indicators are positively correlated with vegetation indices, and are negatively correlated with artificial and thermal indices. The influence of topographic characteristics impacts the variability of LST values, depending on the terrain elevation; in high altitudes where the vegetal cover is dense thermal values are low, unlike low altitudes in the city's center, where thermal values are higher.

Principal component analysis

Before running PCA, the normalized values of all the indicators (environmental, societal, and topographic) were used to examine their suitability for the component analysis using KMO and

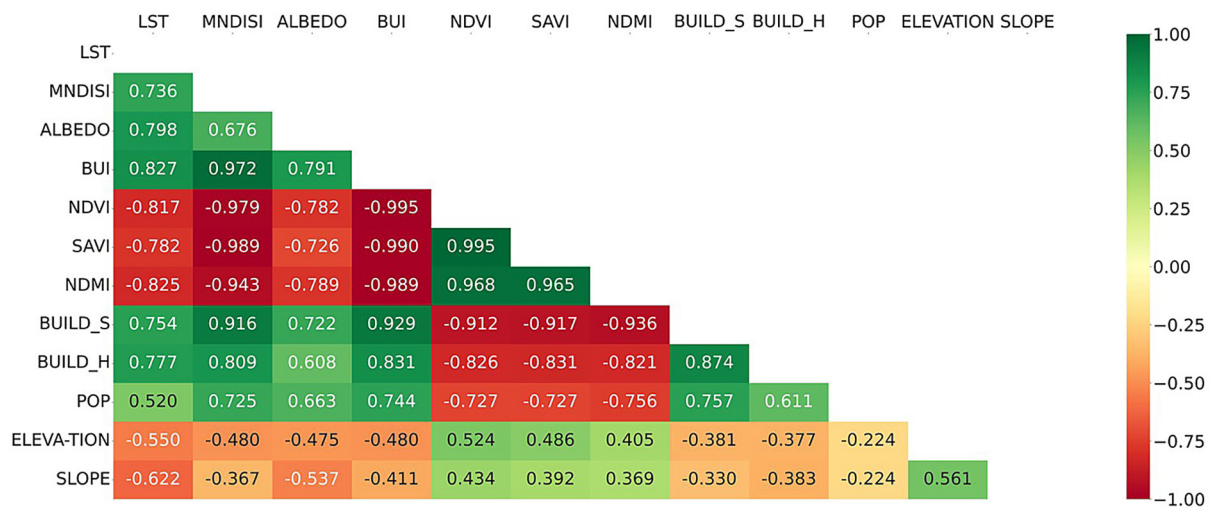


Fig. 4. Pearson correlation matrix among indicators for 2023

Bartlett’s sphericity tests. The data is considered appropriate for PCA only with a KMO value of more than 0.50 and a significant level of Bartlett’s test of less than 0.1. In this study, KMO values were 0.814, 0.807, and 0.826 respectively for 2002, 2013, and 2023. Furthermore, the significant level of Bartlett’s test was 0.000 for the 3 years. These results confirmed the suitability of the indicators for a PCA application in this study [Joseph et al., 2014]. The communality of the selected indicators was then used to evaluate their capacities in the component analysis. Indicators with a communality of less than 0.50 should not be included in the analysis since they are not well representative in the statistical analysis [Iwaniak et al., 2018]. In this study, all the chosen indicators for both years had a communality larger than 0.5. In the PCA technique, only components with eigenvalues higher than 1 should be taken into account [Kaiser, 1960]. In this work, PCA produced three principal components for each year with eigenvalues greater than 1 (Fig. 5), with a total variance percentage of 81.137%, 81.01%, and 81.135% respectively for 2002, 2013, and 2023.

The results show that, in 2002, the first component had strong positive loadings with vegetation indicators, and negative loadings with thermal, impervious surface, and societal indicators (Fig. 5). This component increases with green areas and decreases with the building density and impermeable surfaces. The second component, called the topographic component, has strong and positive scores with topographic indicators (elevation and slope), and low or negative scores with the other indicators. The third

component is correlated with societal indicators, with factor loadings higher than 0.5. In 2013, the first component showed a positive correlation with the societal variables and impervious surfaces, while it had a negative correlation with indicators associated with topographic aspects and vegetation density. The second and third components of 2013 had similar loadings than in 2002. The first component in 2023 shows a positive correlation with greenness and topographic indicators and a negative correlation with built-up and artificial areas. The second component is positively linked to societal indicators, while the third component had positive loadings with topographic parameters.

Urban ecological quality index

All the principal components computed in the above section were combined into one synthetic index by year. The *UEQI* was calculated using the variance percentage of these components in the PCA results for 2002 (Eq. 11), 2013 (Eq. 12), and 2023 (Eq. 13) [Li, 2007]. While the loadings of the vegetation indicators (NDVI, SAVI, and NDMI) were negative in a component, those components were multiplied by (-1) to invert the scores of these indicators. Thus, the *UEQI* index was calculated as follows:

$$UEQI_{2002} = ((58.06 * PC 1) + (12.25 * PC 2 * (-1)) + (10.82 * PC 3))/100 \quad (11)$$

$$UEQI_{2013} = ((58.52 * PC 1 * (-1)) + (12.73 * PC 2 * (-1)) + (9.75 * PC 3))/100 \quad (12)$$

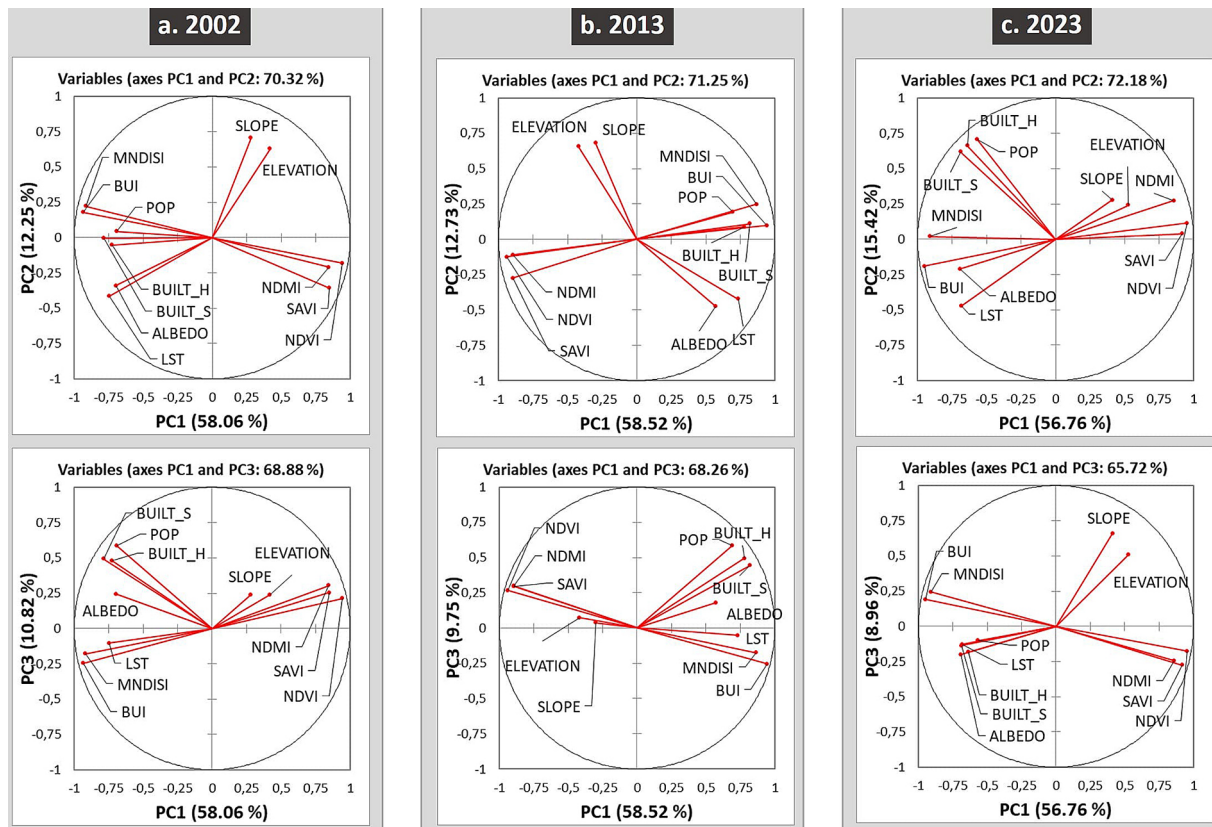


Fig. 5. Principal component analysis results in Tangier city (a. 2002, b. 2013 and c. 2023)

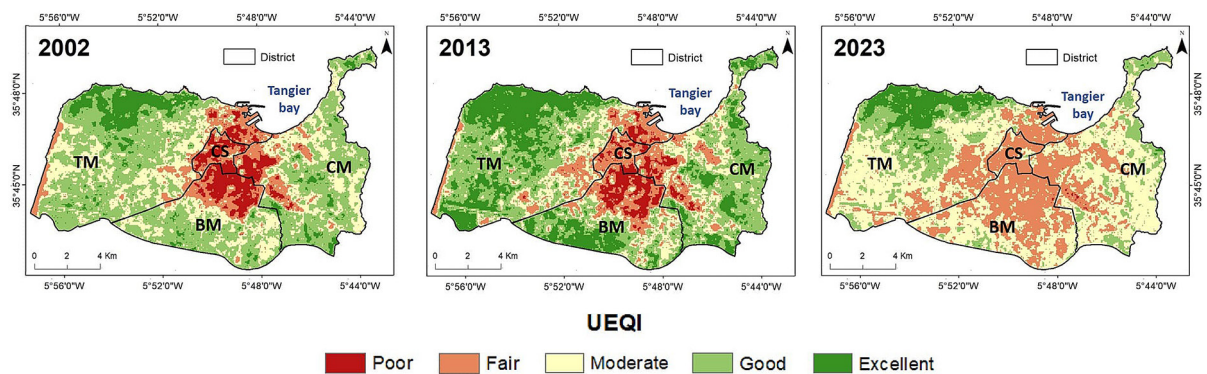


Fig. 6. Spatial distribution of the UEQI in Tangier city for 2002, 2013, and 2023

$$UEQI_{2023} = ((56.76 * PC1) + (15.42 * PC2) + (8.96 * PC3 * (-1))) / 100 \quad (13)$$

For a better representation of UEQI results, the values were normalized [0,1] and then reclassified using 5 classes: poor (UEQI values 0.0 to 0.2), fair (0.2 to 0.4), moderate (0.4 to 0.6), good (0.6 to 0.8), and excellent (0.8 to 1). According to the UEQI results (Fig. 6), the poor ecological quality of the study was mainly located in the north and center of Tangier city, for 2002 and 2013. The northeastern part of TM district, which

is near economic and tourism activity around Tangier bay, the northwestern part of CM district, where the population density is more concentrated, and the CS district, maintain a poor environmental quality for both years. Only agricultural lands and forest zones surrounding the city kept a good UEQI value. However, 2023 is characterized by the decrease of UEQI values in agriculture and vegetation areas, which have been directly impacted by the various drought episodes that Morocco has experienced in the last decade. In general, these findings show that the UEQI values

became poorer approaching Tangier’s center, where there are more artificial areas, low vegetation cover, and high building density. UEQI values became better in the east, west, and extreme south sides when the areas are characterized by high vegetation, high altitude, less impermeable surfaces, and low population density.

Spatial autocorrelation analysis of the UEQI

To conduct a spatial autocorrelation analysis of the UEQI results for 2002, 2013, and 2023, a 100×100 m unit grid was created to cover the three images. A total of 16794 grid cells were generated to extract the values of UEQI and all the other indicators, using the centroid of each grid cell. The same grid cell was used for the three years to ensure a temporal and spatial consistency of results. In this study, the Global Moran’s index of UEQI results was 0.804, 0.784, and 0.761 respectively for 2002, 2013, and 2023, indicating a

strong spatial auto-correlation of UEQI values in Tangier city (Fig. 7). The Global Moran’s scatterplot confirms these findings and shows that there is no random distribution of the UEQI values in the study area for the three studied years.

Positive and negative spatial clustering of UEQI values were mapped using Local Moran’s I cluster maps (Fig. 8), and classified according to their significance level (Fig. 9). The High–High (HH) class means that high UEQI values are spatially surrounded by cells with high UEQI value two. The Low–Low (LL) class represents low UEQI values that are neighboring to other cells with low UEQI values. The High–Low (HL) and Low–High (LH) indicate cells with high value bordering cells with low value, and vice versa. In 2002 and 2013, the (LL) areas indicating poor ecological quality were concentrated in the center, the north, and the extreme west part of the study area, at significance of 0.05, 0.01, or 0.001. In 2023, these (LL) zones spread south of Tangier,

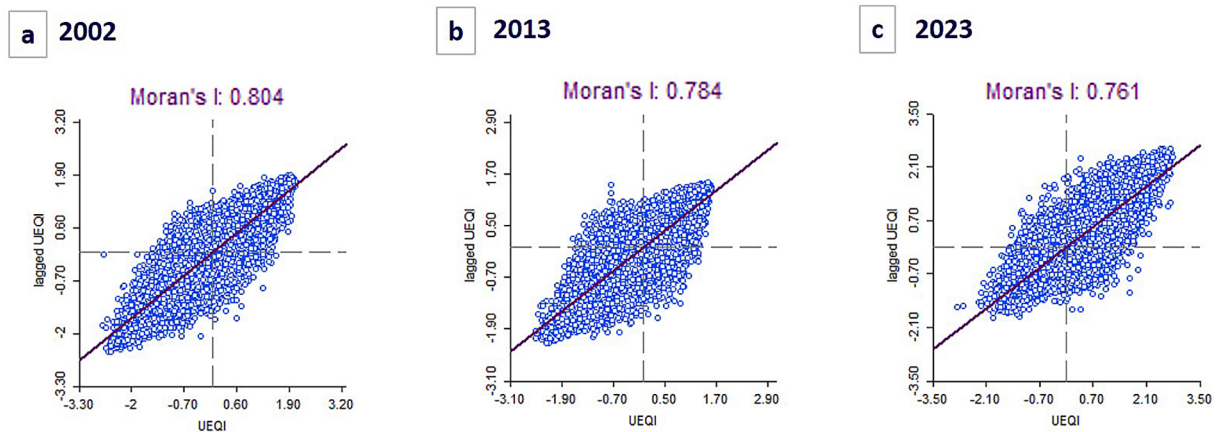


Fig. 7. Global Moran’s results (scatterplot and index value) of UEQI data for 2002, 2013, and 2023 in Tangier city

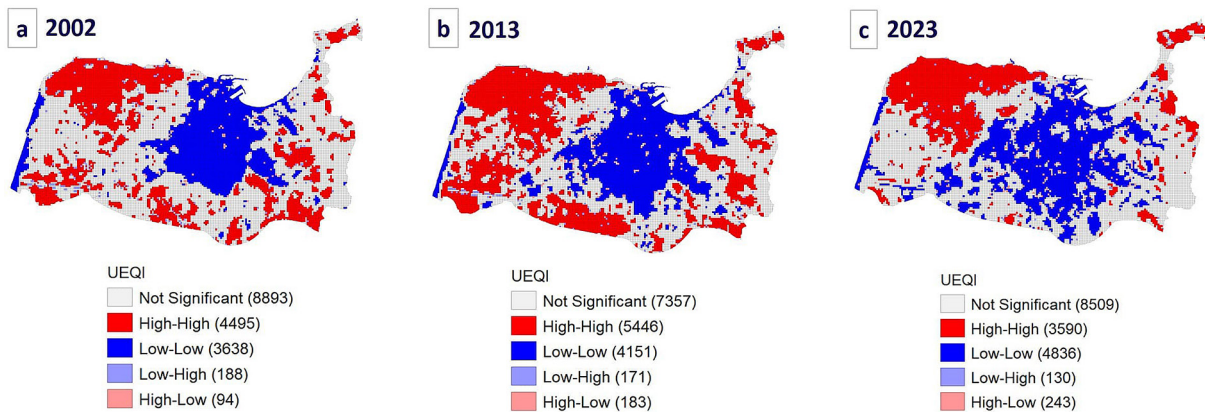


Fig. 8. Local Moran’s I cluster maps of UEQI results for 2002, 2013, and 2023

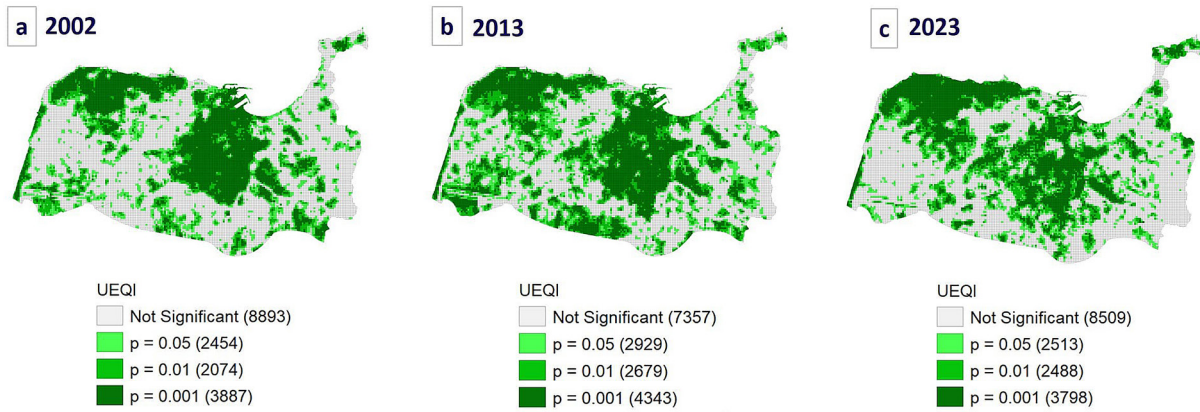


Fig. 9. Significance map of UEQI results for 2002, 2013 and 2023

following the expansion of the city. The HH areas were scattered in the study area during 2002 and 2013 but became more concentrated in 2023 towards the northwest and northeast of the city.

Spatial change detection of the UEQI during 2002–2023

From 2002 to 2013, the spatial change distribution of UEQI classes in Tangier city shows that the urban ecological quality has maintained the same quality as in 2002 in 50% of the study area, improved with scattered enhancements in 36% (Fig. 10). This positive ecological development is due to the precipitation increases that Morocco experienced in this decade. Some classes' degradation (14% of UEQI values) is located in areas that have experienced urban expansion during this decade. However, from 2013 to 2023, UEQI values experienced the greatest degradation, with more than 52% of degraded UEQI, mainly in agricultural and vegetation areas, due to the recent droughts that caused the rising of surface temperature and the lack of greenness areas, but also by

the demographic evolution that spread south of the city. Those findings explain also the spatial changes of the UEQI from 2002 to 2023.

DISCUSSION

Assessing the urban ecological quality in Tangier city, using only remote sensing data, was the main objective of this research. Appropriate and available environmental, societal, and topographic indicators were selected to retrieve the ecological quality of the study area, for the years 2002, 2013, and 2023. PCA technique was used to compute the UEQI index, which identified the major components that depict several aspects of urban ecological quality (green spaces, population density, building surfaces, etc.). The UEQI obtained shows that statistical techniques, such as PCA, can be considered good alternatives for ecological assessment.

The findings of this research showed that building density and green zones are factors influencing urban ecological quality in Tangier

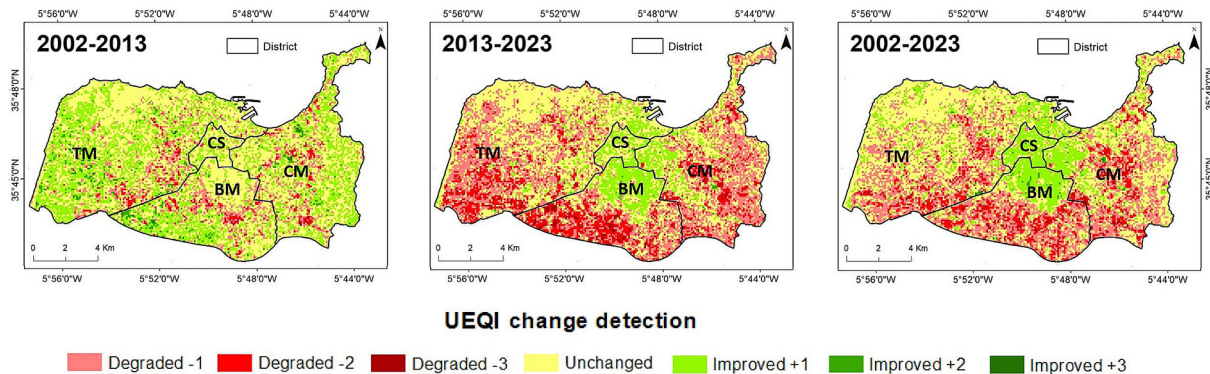


Fig. 10. Spatial change detection of the UEQI in Tangier city for 2002, 2013, and 2023

city. The lack of green vegetation, the presence of impermeable surfaces, and the high population density increase the energy consumption of buildings, impacting the environment negatively. Given the geographical position of the city which is surrounded by high altitudes to the east and west, the city will develop towards the south, mainly in the BM district. To ensure environmental and ecological urbanization in Tangier city, planning measures should be taken in the projected urban areas by involving urban parks [Azyat et al., 2018], and urban and peri-urban agriculture [Fetola et al. 2020] for their environmental benefits.

In existing areas, the urban ecological methodology proposed can allow stakeholders to identify the essential actions to be taken in areas with poor environmental quality. The outcomes findings of this research can also help environmental organizations to identify districts and areas in Tangier city that need further prospection through measures in situ to improve their environmental quality. Moreover, given the demographic projections of the region, authorities and decision-makers should highlight that relocation of the population in poor ecological quality areas, and adoption of supporting legislation might serve as a preventative measure in areas with significant socioeconomic vulnerability, to ensure urban resilience and environmental sustainability. In addition, the development of Tangier's urbanization should be adapted to the climate change impacts, by the implementation of more green cities to improve the urbanized region's ecological quality, such as the Chrafate Green City project, located 18 km southeast of Tangier, which supports the industrial policy of the TTA region for sustainable territorial development. The methodology presented, which is mainly based on remote sensing data, can be applied to other Moroccan (Mediterranean rim) or African cities, where the assessment of the urban quality of life is essential to ensure urban sustainable development.

The outcomes of this study are consistent with the findings of other investigations (especially in other continents). Sousa et al. (2021) highlight the importance of urban afforestation activities in improving the urban environmental quality in a highly urbanized Brazilian city. Roy et al. (2022) consider that developing an urban environmental quality using remote sensing data can serve as a basis for future research and decision-making in India about one of the most important SDGs principles: the development of

sustainable cities. In addition, Pramanik et al. (2021) suggest that the UEQI developed might be used to determine potential local interventions to improve the ecological quality of citizens. According to Musse et al. (2018), despite the lack of data in Latin American cities concerning the urban ecological environment, remote sensing images are considered an excellent data source for analyzing the urban environment quality, since the variables studied can be analyzed and studied through many spatial and temporal scales. In the African context (Assaye et al., 2017), a more sustainable future may be achieved by cities with good urban environmental quality. To aim for this urban sustainability in the European environment, Pawel et al. (2019) recommend the analysis of land cover's possible effects on the urban environmental quality of life in Polish cities, which can be useful in urban greening. The city's urban environmental quality might be impacted by a variety of factors. For this reason, to enhance the consistency of the model proposed, this research can be improved by including demographic and socio-economic data from the next Moroccan census of the population planned for 2024, to better comprehend how socioeconomic factors influence urban sustainability whether in Tangier or another Moroccan city. Furthermore, this research can be improved by analyzing the other seasons and by including more ecological indicators, such as urban air quality, land use/ land cover, urban heat island, and rainfall data, which can be extracted from different satellite imagery.

CONCLUSIONS

Assessing ecological quality in a city using traditional methods is time-consuming, costly, and inefficient. The use of PCA analysis, combined with remote sensing data, has revolutionized the extraction of environmental quality indicators in urban areas. In the present study, the ecological quality of Tangier city was assessed through a combined index, using only remote sensing data, for the years 2002, 2013, and 2023. Three types of indicators were selected for assessing the urban ecological quality: environmental, societal, and topographic indicators. All these parameters were normalized on the same scale [0,1] before PCA analysis. Only components with eigenvalues greater than 1 were kept for this work. The UEQI

Index was then calculated using the score and the variance of each selected component for the three years. To assess the overall spatial pattern of the UEQI, the Global Moran's index varied from 0.761 to 0.804 for the years, suggesting a strong positive spatial auto-correlation of the UEQI results. Furthermore, Local Moran's I cluster maps show that, on the one hand, poor ecological areas were concentrated in Tangier's center in 2002 and then spread south of the city in 2023. On the other hand, green areas, which were highly concentrated around the city in 2002, became highly clustered only in the northwest and northeast of the study area in 2023. In addition, the results show that in 2002, 2013, and 2013, the vegetation cover and the building density were the main reasons for the poor ecological quality of areas located in the center of Tangier city. Agricultural land and green areas were directly affected by the recent droughts periods that Morocco has experienced in recent years. The methodology developed could be replicated for African cities with similar conditions and characteristics since this work provides an integrated approach to interpreting the relationships between all the parameters through spatial visualization of the UEQI. These findings are critical for environmental planners to take the required actions in Tangier's areas with poor ecological quality to improve people's quality of life.

REFERENCES

1. Anselin, L. 1995. Local Indicators of Spatial Association – LISA. *Geographical Analysis*, 27, 93–115. <https://doi.org/10.1111/j.1538-4632.1995.tb00338.x>
2. Artis, D.A., Carnahan, W.H. 1982. Survey of emissivity variability in thermography of urban areas. *Remote Sensing of Environment*, 12(4), 313–329. [https://doi.org/10.1016/0034-4257\(82\)90043-8](https://doi.org/10.1016/0034-4257(82)90043-8)
3. Assaye, R., Suryabhagavan, K.V., Balakrishnan, M., Hameed, S. 2017. Geo-Spatial Approach for Urban Green Space and Environmental Quality Assessment: A Case Study in Addis Ababa City. *Journal of Geographic Information System*, 9, 191–206. <https://doi.org/10.4236/jgis.2017.92012>
4. Azyat, A., Raissouni, N., Achhab, N.B., Chahboun, A., Lahraoua, M., Elmagnougi, I., Sebbah, B., Ismaili, I.A. 2018. Urban Parks Spatial Distribution Analysis and Assessment Using GIS and Citizen Survey in Tangier City, Morocco (2015 Situation). *Advances in Intelligent Systems and Computing*. Vol 915. Springer, Cham. https://doi.org/10.1007/978-3-030-11928-7_55
5. Bahi, H. ; Rhinane, H.; Bensalmia, A.; Fehrenbach, U.; Scherer, D. 2016. Effects of Urbanization and Seasonal Cycle on the Surface Urban Heat Island Patterns in the Coastal Growing Cities : A Case Study of Casablanca, Morocco. *Remote Sensing*, 8(10), Article 10. <https://doi.org/10.3390/rs8100829>
6. Bouramtane, T., Kacimi, I., Bouramtane, K., Aziz, M., Abraham, S., Omari, K., Valles, V., Leblanc, M., Kassou, N., El Beqqali, O., Bahaj, T., Morarech, M., Yameogo, S., Barbiero, L. 2021. Multivariate Analysis and Machine Learning Approach for Mapping the Variability and Vulnerability of Urban Flooding : The Case of Tangier City, Morocco. *Hydrology*, 8(4), Article 4. <https://doi.org/10.3390/hydrology8040182>
7. Chai, N. Mao, C. 2022. Population management in an urban center using the dynamic integrated solution for an adequate atmospheric environmental quality. *Environmental Research*. 205, 112482. <https://doi.org/10.1016/j.envres.2021.112482>
8. Farr, T.G., Kobrick, M. 2000. Shuttle Radar Topography Mission Produces a Wealth of Data. *Eos, Transactions American Geophysical Union.*, 81, 583–585. <https://doi.org/10.1029/EO081i048p00583>
9. Feola, G., Suzunaga, J., Soler, J., Wilson, A.D. 2020. Peri-urban agriculture as quiet sustainability: Challenging the urban development discourse in Sogamoso, Colombia. *Journal of Rural Studies*, 80, 1–12. <https://doi.org/10.1016/j.jrurstud.2020.04.032>
10. Gao, B.-C. 1996. NDWI – A normalized difference water index for remote sensing of vegetation liquid water from space. *Remote Sensing of Environment*, 58(3), 257–266. [https://doi.org/10.1016/S0034-4257\(96\)00067-3](https://doi.org/10.1016/S0034-4257(96)00067-3)
11. He, C., Shi, P., Xie, D., Zhao, Y. 2010. Improving the normalized difference built-up index to map urban built-up areas using a semiautomatic segmentation approach. *Remote Sensing Letters*, 1(4), 213–221. <https://doi.org/10.1080/01431161.2010.481681>
12. High Commissioner for Planning. 2014. General Census of Population and Housing 2014. Regional series of the Tangier-Tetouan-Al Hoceima region.
13. High Commissioner for Planning. 2018. Projections of the population of regions and provinces 2014–2030. https://www.hcp.ma/region-tanger/Projections-de-la-population-des-provinces-et-prefectures-de-la-region-TTA_a322.html
14. Huete, A.R. 1988. A soil-adjusted vegetation index (SAVI). *Remote Sensing of Environment*. 25(3), 295–309. [https://doi.org/10.1016/0034-4257\(88\)90106-X](https://doi.org/10.1016/0034-4257(88)90106-X)
15. Iwaniak, A., Hryniewicz, M., Bucholska, J., Darewicz, M., Minkiewicz, P. 2018. Structural characteristics of food protein-originating di- and tripeptides

- using principal component analysis. *European Food Research and Technology*. 244(10), 1751–1758. <https://doi.org/10.1007/s00217-018-3087-3>
16. Joseph, M., Wang, F., Wang, L. 2014. GIS-based assessment of urban environmental quality in Port-au-Prince, Haiti. *Habitat International*. 41, 33–40. <https://doi.org/10.1016/j.habitatint.2013.06.009>
 17. Kaiser, H.F. 1960. The Application of Electronic Computers to Factor Analysis. *Educational and Psychological Measurement*. 20(1), 141–151. <https://doi.org/10.1177/001316446002000116>
 18. Kamp, I., Leidelmeijer, K., Marsman, G., Hollander, A.E. 2003. Urban environmental quality and human well-being Towards a conceptual framework and demarcation of concepts; a literature study. *Landscape and Urban Planning*. 65, 5–18. [https://doi.org/10.1016/S0169-2046\(02\)00232-3](https://doi.org/10.1016/S0169-2046(02)00232-3)
 19. Kazemzadeh-Zow, A., Bolorani, A.D., Samany, N.N., Toomanian, A., Pourahmad, A. 2018. Spatio-temporal modelling of urban quality of life (UQoL) using satellite images and GIS. *Int. J. Remote Sens.* 39, 6095–6116. <https://doi.org/10.1080/01431161.2018.1447160>
 20. Li, G. 2007. Measuring the Quality of Life in City of Indianapolis by Integration of Remote Sensing and Census Data. *International Journal of Remote Sensing - INT J REMOTE SENS.* 28. <https://doi.org/10.1080/01431160600735624>
 21. Liang, S., Shuey, C.J., Russ, A.L., Fang, H., Chen, M., Walthall, C.L., Daughtry, C.S., Hunt, B.R. 2003. Narrowband to broadband conversions of land surface albedo: II. Validation. *Remote Sensing of Environment*. Volume 84, Issue 1, Pages 25–41. [https://doi.org/10.1016/S0034-4257\(02\)00068-8](https://doi.org/10.1016/S0034-4257(02)00068-8)
 22. Liu, H., Cui, W., Zhang, M. 2022. Exploring the causal relationship between urbanization and air pollution : Evidence from China. *Sustainable Cities and Society*. 80, 103783. <https://doi.org/10.1016/j.scs.2022.103783>
 23. Lo, C.P. 1997. Application of LandSat TM data for quality of life assessment in an urban environment. *Computers, Environment and Urban Systems*. 21(3), 259–276. [https://doi.org/10.1016/S0198-9715\(97\)01002-8](https://doi.org/10.1016/S0198-9715(97)01002-8)
 24. López, E.; Bocco, G.; Mendoza, M.; Duhau, E. 2001. Predicting land-cover and land-use change in the urban fringe : A case in Morelia city, Mexico. *Landscape and Urban Planning*. 55(4), 271–285. [https://doi.org/10.1016/S0169-2046\(01\)00160-8](https://doi.org/10.1016/S0169-2046(01)00160-8)
 25. Malah, A., Bahi, H. 2022. Integrated multivariate data analysis for Urban Sustainability Assessment, a case study of Casablanca city. *Sustainable Cities and Society*. 86, 104100. <https://doi.org/10.1016/j.scs.2022.104100>
 26. Malah, A., Bahi, H., Radoine, H., Maanan, M., Mastouri, H. 2022. Assessment of Urban Environmental Quality: A Case Study of Casablanca, Morocco. *ISPRS – International Archives of the Photogrammetry Remote Sensing and Spatial Information Sciences*, XLVI-4/W3-2021, 205–210. <https://doi.org/10.5194/isprs-archives-XLVI-4-W3-2021-205-2022>
 27. Martin, D., 1996. An assessment of surface and zonal models of population. *Int. J. Geograph. Informat. Syst.* 10, 973–989.
 28. Merschdorf, H., Hodgson, M.E. Blaschke, T. 2020. Modeling Quality of Urban Life Using a Geospatial Approach. *Urban Science*, 4, 5. <https://doi.org/10.3390/urbansci4010005>
 29. Musse, M.A., Barona, D.A., Rodríguez, L.M. 2018. Urban environmental quality assessment using remote sensing and census data. *Int. J. Appl. Earth Obs. Geoinformation*. 71, 95–108. <https://doi.org/10.1016/j.jag.2018.05.010>
 30. Nardo, M., Saisana, M., Saltelli, A., Tarantola, S. 2005. Tools for Composite Indicators Building. EUR 21682 EN. 2005. JRC31473. <https://publications.jrc.ec.europa.eu/repository/handle/JRC31473>
 31. Pacione, M. 2003. Urban environmental quality and human wellbeing—a social geographical perspective. *Landscape and Urban Planning*, 65, 19–30.
 32. Paweł, P., Marek, P., Elżbieta, D. 2019. Evaluation of the location of cities in terms of land cover on the example of Poland. *Urban Ecosystems*, 22, 619–630. <https://doi.org/10.1007/s11252-019-00848-8>
 33. Pesaresi, M., Politis, P. 2022a. GHS-BUILT-S R2022A - GHS built-up surface grid, derived from Sentinel2 composite and Landsat, multitemporal (1975-2030). European Commission, Joint Research Centre (JRC). <https://doi.org/10.2905/D07D81B4-7680-4D28-B896-583745C27085>
 34. Pesaresi, M., Politis, P. 2022b. GHS-BUILT-H R2022A - GHS building height, derived from AW3D30, SRTM30, and Sentinel2 composite (2018). European Commission, Joint Research Centre (JRC). <https://doi.org/10.2905/CE7C0310-9D5E-4AEB-B99E-4755F6062557>
 35. Pramanik, S., Arendran, G., Punia, M., Sahoo, S.K. 2021. Spatio-temporal pattern of urban eco-environmental quality of Indian megacities using geo-spatial techniques. *Geocarto International*. 37, 5067–5090. <https://doi.org/10.1080/10106049.2021.1903578>
 36. Roy, S., Bose, A., Majumadar, S., Roy Chowdhury, I., Abdo, H.G., Almohamad, H., Abdullah Al Dughairi, A. 2022. Evaluating urban environment quality (UEQ) for Class-I Indian city: An integrated RS-GIS based exploratory spatial analysis. *Geocarto International*. <https://doi.org/10.1080/10106049.2022.2153932>
 37. Schiavina, M., Freire, S., MacManus, K. 2022. GHS-POPR2022A - GHS population grid multitemporal (1975–2030). European Commission, Joint

- Research Centre (JRC). <https://doi.org/10.2905/D6D86A90-4351-4508-99C1-CB074B022C4A>
38. Sousa, J.A., Sales, J.C., Silva, D.C., Silva, R.C., Lourenço, R.W. 2021. Developing Of An Urban Environmental Quality Indicator. *Geography, Environment, Sustainability*, Vol.14, No 2, p. 30–41. <https://doi.org/10.24057/2071-9388-2020-210>
39. Sun, Z., Wang, C., Guo, H., Shang, R. 2017. A Modified Normalized Difference Impervious Surface Index (MNDISI) for Automatic Urban Mapping from Landsat Imagery. *Remote. Sens.*, 9, 942. <https://doi.org/10.3390/rs9090942>
40. Tucker, C.J. 1979. Red and photographic infrared linear combinations for monitoring vegetation. *Remote Sensing of Environment*, 8(2), 127–150. [https://doi.org/10.1016/0034-4257\(79\)90013-0](https://doi.org/10.1016/0034-4257(79)90013-0)
41. UN. 2007. State of World Population 2007. United Nations Population Fund. <https://www.unfpa.org/publications/state-world-population-2007>
42. UN. 2010. State of African Cities 2010 , Governance, Inequalities and Urban Land Markets | UN-Habitat. <https://unhabitat.org/state-of-african-cities-2010-governance-inequalities-and-urban-land-markets-2>
43. UN. 2022. World Population Prospects – Population Division, United Nations. <https://population.un.org/wpp/>
44. Weng, Q. 2012. Remote sensing of impervious surfaces in the urban areas : Requirements, methods, and trends. *Remote Sensing of Environment*. 117, 34–49. <https://doi.org/10.1016/j.rse.2011.02.030>
45. World Bank. 2021. Morocco | Data. <https://data.worldbank.org/country/MA>
46. Xu, H. 2006. Modification of Normalized Difference Water Index (NDWI) to Enhance Open Water Features in Remotely Sensed Imagery. *International Journal of Remote Sensing*, 27, 3025–3033. <https://doi.org/10.1080/01431160600589179>